

Lack of time-dilation in type Ia supernovae and Gamma-Ray Bursts

DAVID F. CRAWFORD

Astronomical Society of Australia, 44 Market St., Naremburn NSW, 2065, Australia

(Received October 16, 2018; Revised October 17, 2018; Accepted December 3, 2024)

Submitted to ApJ

ABSTRACT

A fundamental property of an expanding universe is that any time interval of the characteristics of distant objects must appear to scale by the factor $(1+z)$. This is called time-dilation. Light curves of type Ia supernovae and the duration of Gamma-Ray Bursts (GRB) are the only observations that can directly measure time-dilation over a wide range of redshifts. An analysis of raw observations of 2,133 type Ia supernovae light-curves shows that their widths are proportional to $(1+z)^{(-0.038 \pm 0.075)}$ which is consistent with no time-dilation and inconsistent with standard time-dilation. Analysis of the duration of GRB shows that they are consistent with no time-dilation and have very little support for standard time-dilation. In addition, it is shown that the standard method for calibrating the type Ia supernovae light-curves (SALT2) is flawed, which explains why this lack of time-dilation has not been previously observed.

Keywords: Cosmology: large-scale structure of the universe–Cosmology:general–Supernovae: miscellaneous

1. INTRODUCTION

Nearby type Ia supernovae are well known to have essentially identical light-curves that make excellent cosmological probes. It is argued in Section 2 that the only characteristics of the light-curve that change with redshift are the scaling parameters of peak luminosity and width. Here the interest is in the width which must vary with redshift in exactly the same way as time-dilation. For an expanding universe the relative width must be proportional to $(1+z)$, and for a static universe, it must be constant.

In Section 3 it is argued that in quantum mechanics the apparent wavelength of a photon is a measurement of its energy and as a consequence redshifts may be due to any process that causes a loss of energy. Thus in quantum mechanics the rigid nexus between the shift of spectral lines and the shift of other time variations is broken.

The observational evidence for standard time-dilation has a long history with notable papers being Goldhaber et al. (2001) and Blondin et al. (2008). The observed width of any light-curve from a distant object is the product of an intrinsic width with the width due to time-dilation. The intrinsic width is a function of the intrinsic (rest-frame) wavelength which is shorter than the observed wavelength. Since many of the intrinsic wavelengths are outside the visible range its width spectrum cannot be easily determined from nearby supernovae. A suitable method of solving this problem is to generate a reference template that provides a complete light-curve for each intrinsic wavelength, and then to use these templates to accurately calibrate the observations by eliminating any intrinsic effects.

The SALT2 method (Guy et al. 2007, 2010) determines these templates by combining a large number of observations over a wide range of redshifts and has been used by Betoule et al. (2014), Conley et al. (2011), Foley et al. (2018), Scolnic et al. (2017) and Jones et al. (2018). In other words, the reference template is the average of the light-curves from many supernovae as a function of intrinsic wavelength.

It has been shown by Crawford (2017) and here in Section 4.1 that there is a fundamental problem with this analysis in that a systematic variation in width as a function of redshift is included in the template as a systematic variation of the width as a function of intrinsic wavelength. It is shown that the SALT2 calibration process is very good at removing the intrinsic variations but at the same time, it removes systematic redshift variations such as time-dilation. Thus supernovae light-curves that have been calibrated by SALT2, or a similar method, have all the cosmological information that is a power-law function of redshift removed. In particular any time-dilation is removed from the calibrated widths.

A major part of this paper (Section 5) is an examination of the raw observations for 2,133 supernovae to investigate how the widths of their light-curves vary with redshift. This is done in three stages. The first is to compare the average light-curves for four different redshift ranges. Secondly, it is shown that an analysis of the raw observations as a function of intrinsic width shows a small power-law dependence. Because of a direct correspondence between redshift power-laws and intrinsic wavelength power-laws (Section 4.1) this shows that there little likelihood that the widths have a significant cosmological redshift dependence.

Finally, a direct power-law fit of the light-curve widths of type Ia supernovae with redshift shows that the widths are proportional to $(1+z)^{(-0.038 \pm 0.075)}$ which is consistent with no time-dilation.

Gamma-Ray Bursts (GRB) are the only other observations that can provide direct measurements of time-dilation over a wide range of redshifts. The analysis used here (Section 6) investigates the observed durations of the bursts as a function of redshift and again finds that they are consistent with no time-dilation.

It is assumed for this analysis that the intrinsic properties of the type Ia supernovae light-curves and the GRB burst durations are the same at all redshifts.

2. COSMOLOGICAL CHARACTERISTICS OF LIGHT-CURVES

Let us assume that the intrinsic radiation characteristics of type Ia supernovae (or any other object) are independent of redshift and that in an expanding universe the rate of universal expansion is constant for the duration of the light-curve. Since cosmology only controls the transmission of the light, it follows that the shape of the received light-curve must be the same as the shape of the intrinsic light-curve but with different scale factors. In other words, the cosmology can only change the peak flux density and the width of the light-curve. Conse-

quently, all of the cosmological information is contained in the dependence of these two variables with redshift. Thus, it is only necessary to measure these two scaling parameters in order to investigate the cosmology of light-curves.

3. REDSHIFTS AND TIME-DILATION

The Hubble redshift law states that distant objects appear, on average, to have an apparent velocity of recession that is proportional to their distance. Since this is consistent with models of an expanding universe in General Relativity that have universal expansion, such expanding models have become the standard paradigm. Classically, this redshift was obvious because in these models spectral lines are shifted in wavelength exactly like any other time-dependent phenomena.

However quantum mechanics tells us that light is transmitted by photons whose effective wavelength is determined from their momentum by the de Broglie equation $\lambda = hc/E$ where E is their energy and λ is their effective wavelength. Thus their effective wavelength is simply a measurement of their energy and is not a proper wavelength in the classical sense. Nevertheless it does describe how photons can be diffracted and their energy measured by an interferometer. The Doppler effect and the universal expansion are explained by an actual loss (or gain) of energy. A consequence is that redshifts may be due to any process that causes a loss of energy. Thus in quantum mechanics, the rigid nexus between the shifts of spectral lines and the shifts of other time variations is broken.

4. THE INTRINSIC WAVELENGTH DEPENDENCE OF LIGHT-CURVE WIDTHS

Observations of local type Ia supernovae show that the emission from the expanding gas cloud is multi-colored and the intensity is a function of both wavelength and time. A major practical problem is that the emitted wavelengths are often much shorter than the observed wavelengths and since the shape and size of the intrinsic light-curve is a function of the wavelength the analysis of observations requires that this intrinsic dependence is known. For high redshift supernovae, many of the emitted wavelengths are outside the visual range, which means that we cannot use nearby supernovae to obtain the required calibrations.

An ingenious solution, exemplified by the SALT2 method (Guy et al. 2007, 2010), is to determine the calibration spectra from averaging the light-curves of many supernovae at many different redshifts. Because the only observations available are from filters that cover a large wavelength range this is a difficult process. This

and similar methods carefully de-construct the average light-curves, as a function of intrinsic wavelength from a large number of observations, and then generate a light-curve template for each intrinsic wavelength. Thus the light-curve for any particular intrinsic wavelength will have contributions from supernovae at many observed wavelengths.

The observed width of the light-curve is the product of the intrinsic width and the cosmological width. If each can be described by a power-law then the observed width at the observed wavelength λ is

$$w(\lambda) = (1+z)^\alpha \epsilon^\beta \quad (1)$$

where $\epsilon = \lambda/(1+z)$ is the intrinsic wavelength of the observation. By definition, the redshift, z , is defined by $\lambda = (1+z)\epsilon$ and is usually measured from the observed wavelength shift of emission or absorption lines.

4.1. A flaw in the SALT2 Method

However, there is a problem described by Crawford (2017) with the SALT2 method of determining the characteristics of the intrinsic light-curve. Let $w(\lambda)$ be the observed width at wavelength λ and let $W(\epsilon)$ be the width at the intrinsic (rest-frame) wavelength ϵ . (The use of w and W was chosen to mimic the familiar use of m and M for magnitudes.) Similarly, let $f(\lambda)$ and $F(\epsilon)$ be the observed and emitted flux densities.

It is obvious that if the intrinsic flux density is a power-law function of wavelength, that is $F(\epsilon) \propto \epsilon^\beta$, then $f(\lambda) \propto \lambda^\beta (1+z)^{-\beta}$ which shows that there is a close correspondence between a systematic variation in width with intrinsic wavelength and time-dilation. Although this is interesting, the extension to a wide range of observed wavelengths needs a more refined analysis. Here it is assumed that there is no cosmological width dependence, that is $\alpha = 0$

The supernovae observations typically consist of the flux density measure in filters that essentially cover the visual wavelengths. Since each filter has filter gain function, $g(\lambda)$ which is the fraction of power transmitted per unit wavelength, then the flux density observed by a particular filter at the wavelength λ is given by

$$f(\lambda, z) = \int g(\lambda^*) F(\epsilon) d\lambda^*. \quad (2)$$

Now the width of the light-curve is determined by comparing the epoch of an observed flux density to the epoch of a template light-curve which has the same relative flux density. Since this process is a linear function of the flux densities, equation 2 can be applied to the

widths to get

$$w(\lambda, z) = \int g(\lambda^*) W(\epsilon) d\lambda^*. \quad (3)$$

Now suppose the intrinsic light-curves have a power-law wavelength dependence so that $W(\epsilon) = \epsilon^\beta$ where β is a constant. Then including this power-law in equation 3 gives

$$w(\lambda, z) = \int g(\lambda^*) \left(\frac{\lambda^*}{1+z} \right)^\beta d\lambda^*. \quad (4)$$

Since the $(1+z)$ term is independent of λ^* it can be taken outside of the integral to get

$$w(\lambda, z) = A(1+z)^{-\beta}, \quad (5)$$

where

$$A = \int g(\lambda) \lambda^\beta d\lambda. \quad (6)$$

Since A is only a function of β and the filter characteristics, it is the same for all observations with this filter. Consequently, if the intrinsic widths have a power-law dependence on wavelength, proportional to ϵ^β this will be seen as a power-law dependence of the observed widths that is proportional to $(1+z)^{-\beta}$.

Conversely, if there is no intrinsic variation of the widths of the light-curve with wavelength but there is a time-dilation with exponent α , then the derived intrinsic wavelength dependence in the template from multiple supernovae will have a power-law dependence with $\beta = -\alpha$. Note that this is consistent with equation 1 since the usual requirement is to determine

$$w_{\text{cosmological}} = w_{\text{observed}}/w_{\text{intrinsic}} \quad (7)$$

In practice, this means that during the generation of a reference spectrum, any observed time-dilation is recorded in the templates as an intrinsic wavelength dependence. When this is used to calibrate new observations that (by definition) have the same time-dilation, this redshift dependence in the observations will be canceled by the wavelength dependence in the template and the calibrated widths will be independent of redshift.

Consequently, if the SALT2 or similar calibration method is used then any cosmological information that was in the calibration observations in the form of a power-law of $(1+z)$, will be removed from subsequent analyzes. Simply put, the SALT2 calibration removes all power-laws as function of $(1+z)$, whether artificial or genuine, leaving the calibrated light-curve without any power law information.

4.2. SALT2 template analysis

In order to remove the expected time-dilation, the first step of the SALT2 analysis is to divide all the epoch differences by $(1+z)$. If there is no time-dilation this will produce an effective time-dilation of $(1+z)^{-1}$. Figure 1 shows the relative width (in blue and yellow points) for each wavelength of the widths of the light-curves in the SALT2 template (c.f. appendix A). Since there are clearly problems with some of the widths, shown in yellow, the analysis was confined to the blue points. The explanation for the bad widths is unknown but one contributing factor could be poor data available for wavelengths between the filters. Shown in Figure 1 are some filter response curves for the nearby supernovae where this effect would be most pronounced.

The blue line is the best power-law fit of the blue points and has an exponent of 1.240 ± 0.011 . Because the original data obtained from observations with very wide filters there is a large correlation in the width between nearby wavelengths. Thus the uncertainty estimate in this exponent is probably too small.

This observed redshift wavelength dependence can be explained either by there being no time-dilation and an intrinsic dependence with exponent 0.240, or that it has the standard time-dilation and a large intrinsic dependence with exponent 1.240. Note that if there is no time dilation and the effects of auxiliary parameters are small, then the SALT2 stretch factors are estimates of the true width.

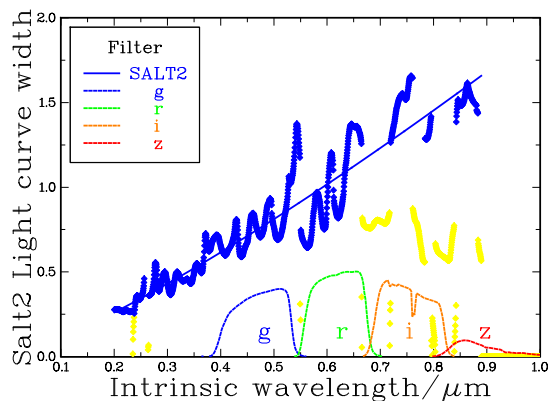


Figure 1. A plot, in blue, of the relative widths of the light-curves for the SALT2 templates as a function of intrinsic wavelength. The blue line is the best fit power-law with an exponent 0.240 ± 0.014 . Yellow points are assumed to be invalid. For comparison some of the filter response curves for nearby supernovae are also shown.

5. TYPE IA SUPERNOVAE LIGHT-CURVES

5.1. The reference template

The essential aim of this analysis is to determine α and β in equation 1, by examining the raw observations of type Ia supernovae. A critical part of any investigation into type Ia supernovae light-curves is to have a reference template. Although the shape of the template is clearly dependent on intrinsic wavelength it has been argued that the effects of time-dilation do not change its shape: they only change the scaling parameters. Thus all we require from the intrinsic properties of the light-curve is the width and peak flux density as a function of intrinsic wavelength in order to distinguish intrinsic properties from cosmological properties.

Although I could use an average template from the raw supernovae data, I decided that in order to remove any possible bias, it would be better to use a standard independent template, the *B* band Parab-18 from Table 2 Goldhaber et al. (2001). Then my procedure is (for each supernova) to determine the observed width of the light-curve for each filter and then independently estimate α and β using equation 1.

5.2. The raw observations

Crawford (2017) describes the selection and analysis of the original observations of type Ia supernovae light-curves that have been selected by Betoule et al. (2014), who have provided an update of the Conley et al. (2011) analysis with better optical calibrations and more supernovae. This JLA (Joint Light-curve Analysis) list sample has 720 supernovae from the Supernova Legacy Survey (SNLS), nearby supernovae (LowZ), the Sloan Digital Sky Survey (SDSS) (Holtzman et al. 2008; Kessler et al. 2009) and those observed by the (HST) (Hubble Space Telescope) (Riess et al. 2007; Jones et al. 2013). Also included are 1169 supernova from the Pan-STARRS supernova survey (Kaiser et al. 2010; Jones et al. 2018; Scolnic et al. 2018). The sources of the raw observations are listed in appendix A.

For each type Ia supernovae, the data used here was, for each filter, a set of epochs with calibrated flux densities and uncertainties. The observations taken with the *U* and *u* filters are very noisy, and following Conley et al. (2011) and Betoule et al. (2014), the observations for these filters were not used.

5.3. The analysis of raw observations

Figure 2 shows the light-curves for four filters for the SNLS supernova SN2007af with the filters used being shown in the legend (Goobar & Leibundgut 2011). Accepted data points are shown as a solid diamonds whereas the rejected points are shown with an open

crossed circle. The first feature to notice is that the epoch of the peak flux density depends on the filter type and is therefore a function of the intrinsic wavelength. Secondly, there is a secondary peak at about 30 days after the first peak for the longer wavelength filters. Although this second peak is intrinsic to the supernova it does not appear to be very consistent (Elias et al. 1981; Meikle & Hernandez 2000; Goobar & Leibundgut 2011). Consequently, as shown in Figure 2, all filters, except *B*, *j*, and HST, had their epochs more than 12 days after the main peak rejected. Note that other epochs were rejected during the analysis.

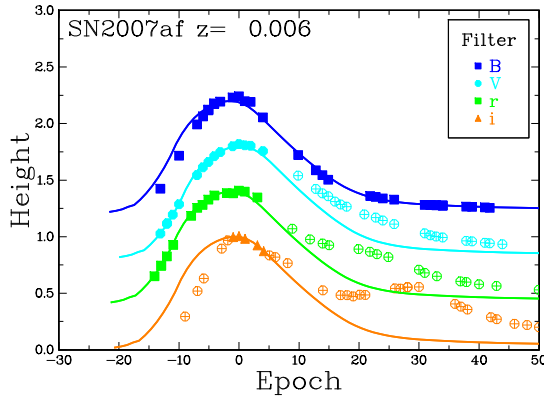


Figure 2. The light-curves for the SNLS type Ia supernova SN2007af. Valid points are shown as full squares and invalid points as open crossed circles. The secondary peak is clearly apparent.

The aim of the analysis for each supernova and filter was to estimate relative width of its light-curve. To do this the first step of the process was a determination of the position and size of the peak flux density. This was done by finding the peak flux density, that minimized the average χ^2 of the flux densities at the accepted epochs as a function of peak position.

Although all the flux densities had uncertainties, for some supernovae these uncertainties were systematically too small or too large. This problem was overcome by only using the relative size of the uncertainties to provide weighting factors. In particular the determination of outliers was done by comparing the χ^2 value for each epoch with the average of the χ^2 values of all the other accepted epochs for the same filter and supernova. It was rejected if its χ^2 value was greater than five times the rms χ^2 of the other values. In order to try and avoid mutual effects the epoch with the largest difference was eliminated and then the analysis was repeated until there were no more eliminations. The end result was a list of accepted epochs and their relative flux density.

The second step was, for each valid epoch, to determine the “flux density” epoch, which is the epoch in the template that has the same relative flux density as the observed epoch. Its uncertainty is proportional to the relative flux density uncertainty divided by the absolute value of the slope of the light-curve at that epoch. A weighted regression between the actual epochs and the flux density epochs for all filters provide an estimate of the width of the supernova light-curve and its uncertainty. Note that the uncertainty in the width is determined by the goodness of fit and only assumes that the original uncertainties were valid except for an unknown common scaling factor.

5.4. Redshift dependence of light-curves

The observed light-curve for each of four redshift ranges was computed for each epoch in the range from -15 days to 40 days from the peak flux density epoch. This was done by selecting all relative flux densities that were within three days of this epoch and setting the value of the light-curve to be the median relative flux density. The median was used because it is insensitive to extreme values. This method depends only on the relative flux density for each epoch and does not depend on the fitted widths.

The results are presented graphically in Figure 3 which shows the average light-curves for four ranges of redshift. The black curve shows the master template light-curve. Table 1 shows the redshift range, the mean redshift, the number of points, and the average width for each range.

Table 1. Light curve widths for four redshift ranges

Range	\bar{z}^a	number	Exponent
0.00-0.15	0.05	26	1.20 ± 0.12
0.15-0.30	0.25	26	0.90 ± 0.12
0.30-0.50	0.39	26	0.85 ± 0.12
0.50-1.30	0.65	26	1.31 ± 0.07

^aThe average redshift

There is no significant variation of the width with redshift and thus they consistent with no time-dilation. Note that if there was standard time-dilation the highest redshift range has an expected width of 1.65.

5.5. Intrinsic widths

Figure 4 shows a plot of all 1,070 supernovae filter widths that had an uncertainty less than 0.1, as a function of their intrinsic wavelength. This is similar to the

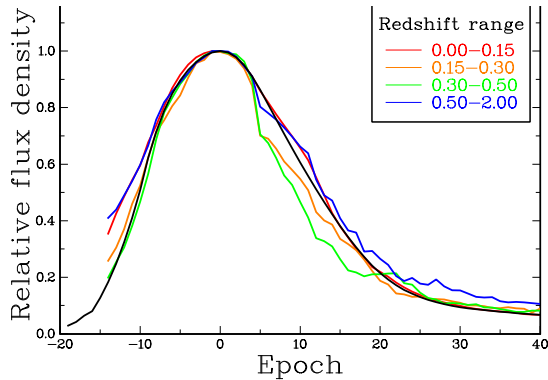


Figure 3. The type Ia supernovae light-curves for four redshift ranges. The legend shows the color for each redshift range. The template light-curve is shown in black. Clearly, there is no systematic change in width with redshift.

type of analysis done by Goldhaber et al. (2001) and Blondin et al. (2008). A power-law fit to these points as a function of intrinsic wavelength provides the estimate $\beta = 0.171 \pm 0.055$. Even though this is marginally significant it is in agreement with the SALT2 value $\beta = 0.240 \pm 0.011$.

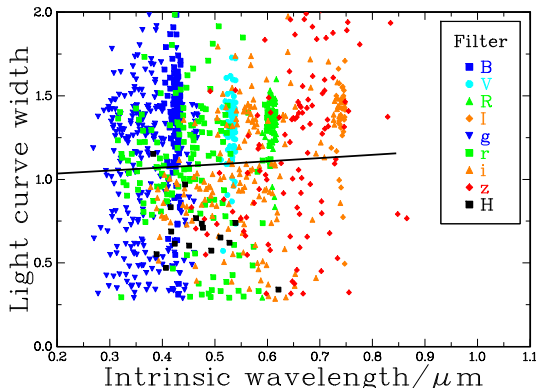


Figure 4. A plot of 1,070 type Ia supernovae filter widths as a function of intrinsic wavelength. The legend shows the filter color and symbol of the supernovae widths for each range. The fitted power-law of the width as a function of wavelength, with exponent $\beta = 0.171 \pm 0.055$, is shown in black.

5.6. Cosmological widths

There were 3502 separate estimates for the width of the supernova light-curve and its uncertainty. From these 1,070 that had a width uncertainty less than 0.1 were selected for analysis. The choice of the 0.1 width uncertainty limit was a compromise between selecting the best observations and having a large number of observations. This limit is not critical and values between 0.02 and 0.25 gave essentially the same results. A power-

law fit all these widths as a function of $(1+z)$ gives an exponent $\alpha = -0.138 \pm 0.076$ which is consistent with zero. If the observations are corrected for the intrinsic width, $\beta = 0.171$, the exponent is $\alpha = 0.038 \pm 0.075$. These results are inconsistent with standard time-dilation and are consistent with no time-dilation.

This conclusion is supported by Figure 5 which shows the distribution of these widths as a function of redshift. There were 17 out of 33 HST supernovae that had width uncertainties less than 0.1 and were thus included in the power-law fit. Except for 4 widths which had too few observations to provide reliable width uncertainties, their uncertainties are shown in Figure 5.

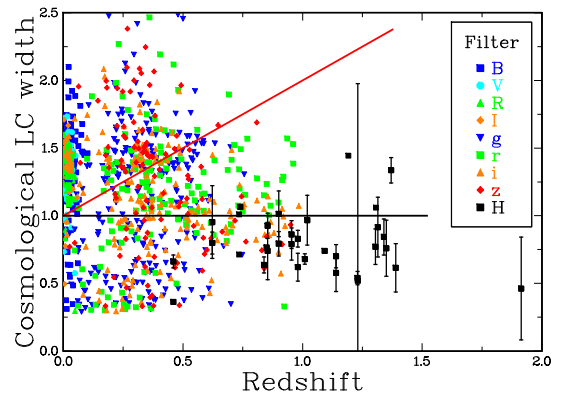


Figure 5. A plot of the measured width of the light-curve for each type Ia supernova as a function of redshift that has a width uncertainty less than 0.1. The black line shows the width for $\alpha = 0$ and the red line shows the width for $(\alpha = 1)$. The symbol and color for each filter are shown in the legend. The HST observations are shown in black. Uncertainties are shown for HST widths that had valid uncertainties.

5.7. A supernova with $z = 1.914$

Jones et al. (2013) describe the observation with the HST of a supernova at a redshift 1.914. They analyzed the data and found a SALT2 width of 1.367 which corresponds to a stretch factor of 0.469. It has been argued in Section 4.1 that the SALT2 method is flawed, therefore these values are flawed. My analysis of the data in their Table 1 provides a width of 0.38 ± 0.32 which is in agreement with their stretch factor. This result is shown in Figure 5. Although its small width may be due to statistical fluctuations, it may be due to an incorrect identification as a type Ia supernova. Their SALT2 analysis played an important part in its identification.

6. GAMMA RAY BURSTS

The website of the *Neil Gehrels* Swift Observatory, which runs the Swift satellite, that contains the Burst

Alert Telescope (BAT) describes GRB as: “Gamma-ray bursts (GRBs) are the most powerful explosions the Universe has seen since the Big Bang. They occur approximately once per day and are brief, but intense, flashes of gamma radiation. They come from all different directions of the sky and last from a few milliseconds to a few hundred seconds.” An important characteristic of the BAT is that it has a photon counting detector (Barthelmy et al. 2005) that detects photons in the 15–150 keV energy range with a resolution of about 7 keV. It can also image up to 350 keV without position information. An important parameter for each burst is T_{90} which is a measure of the burst duration. The start and end times of T_{90} are defined as the times the fraction of photons in the accumulated light-curve reaches 5% and 95%.

The Third Swift Burst Alert Telescope Gamma-Ray Burst Catalog (Lien et al. 2016) states that “Many studies have shown that the observed burst durations do not present a clear-cut effect of time-dilation for GRBs at higher redshift.” Indeed the upper panel of their Figure 25 shows that there is no obvious trend of the burst length with redshift except for a decrease in the number of short bursts with larger redshifts. This shows some support for the “tip-of-the-iceberg” effect which is sometimes used to explain the lack of strong time-dilation in the GRB durations. However, there is no obvious change in the duration of longer bursts with redshift.

Now the number distribution of photons in GRB bursts is close to a power-law with an exponent of about -1.6. As the redshift increases, the number of detectable photons will rapidly decrease as many photons will be below the detector limit. If we assume that the distribution of photons as a function of energy is independent of the position of the photon in the burst, then there should be no expected change in T_{90} with redshift. On the other hand, if the higher energy photons are clustered towards the center of the GRB then the intrinsic T_{90} should decrease with increasing redshift. Consequently, we would expect to see the normal time-dilation or maybe a little less in the T_{90} measurements.

This analysis directly examines the exponent of a power-law regression of measured T_{90} of raw GRB data (c.f. Appendix B), that had burst durations above 2 seconds, as a function of $(1+z)$. Since there were no T_{90} uncertainties provided, the analysis used an unweighted regression. The power-law fits were done for the T_{90} duration with the exponent shown in row 1 of Table 2 which is consistent with no time-dilation. The problem with this and similar analyzes is that the variables have a very large scatter in values which would require very

large numbers of GRB to achieve absolutely conclusive results.

In a recent analysis Zhang et al. (2013) claim that the GRB T_{90} widths are consistent with an expanding universe. They measured T_{90} in the observed energy range between $140/(1+z)$ keV and $350/(1+z)$ keV, corresponding to a fixed energy range in the intrinsic energy range of 140–350 keV. Their exponent is 0.94 ± 0.26 which is consistent with the standard expanding model.

My re-analysis of their raw, T_{90} widths using the data in their Table 1, is shown in columns 2 and 3 of Table 2 are consistent with no time-dilation. The two sets of T_{90} widths are displayed in Figure 6. Although they have many common GRB there are small differences in the T_{90} widths. This is because Zhang et al. (2013) have used their own analysis of the original data to get their own values for T_{90} widths. Examination of Figure 6 shows the large scatter of the T_{90} widths and it also shows that they are consistent with no time-dilation and are unlikely to be consistent with standard time-dilation.

My determination of the exponents of their energy selected widths as a function of $(1+z)$ is shown in rows 4 and 5 of Table 2. The unweighted result in row 4 agrees with their result. However the exponent for the weighted analysis shown in row 5 is consistent with no time-dilation.

The use of a “k correction” for T_{90} implies that there is an intrinsic dependence of burst duration on the photon energy. Since the BAT has a photon counting detector, any measurement of T_{90} is independent of the selected photon energies. The only restriction is that the photon energies must be within the detector limits. Thus BAT does not have the energy selection that is necessary for this “k correction”. Furthermore it is difficult to understand how a subset of photons can have a different time-dilation from the rest of the photons in the same GRB. If we ignore the Zhang et al. (2013) results, the conclusion is that burst lengths of GRB are consistent with no time-dilation and have very little support for the standard model.

7. SUMMARY

7.1. Supernovae

The first part of this paper argued that the only effects of cosmology on supernovae light-curves is to change the scaling parameters of peak flux density and width. The shape of the light-curve is intrinsic to the supernovae and is unchanged by cosmology.

Next, it was argued that the redshift of photons is a measure of their energy and could be caused by any systematic energy loss or by time-dilation.

Table 2. Exponents for redshift dependence of GRB

Row	Data	Weight ^a	N	Exponent
1	Swift	U	298	0.39 ± 0.17
2	Zhang ^b	U	139	0.10 ± 0.26
3	Zhang ^b	W	139	-0.16 ± 0.20
4	Zhang ^c	U	139	0.94 ± 0.26
5	Zhang ^c	W	139	0.31 ± 0.23

^aU denotes an unweighted fit, W denotes a weighted fit

^bRaw T_{90} provided by Zhang et al. (2013) in Table 1

^c $T_{90,z}$ for intrinsic energy range of 140-350 keV

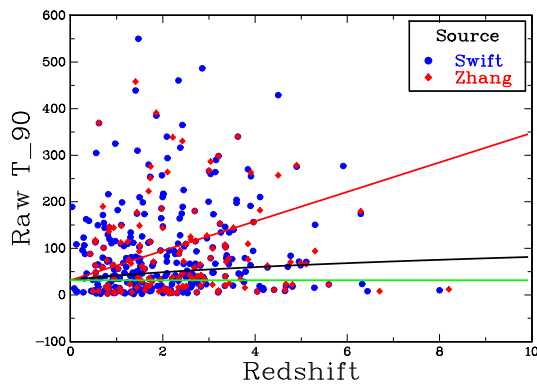


Figure 6. A plot of T_{90} as a function of redshift. The green line shows the line for no time-dilation, the red line shows the line for standard time-dilation, and the black line shows a time-dilation with the fitted exponent of 0.39. The Swift data are shown in blue filled circles and the Zhang (Zhang et al. 2013) data are shown as red diamonds.

In Section 4.1 and 4.2 it has been shown that there is a major problem in using SALT2, and similar calibration methods, to remove the intrinsic wavelength dependence of widths from type Ia supernovae light-curve observations. The process of generating the templates means that if the observed light-curves have widths that contain the effects of time-dilation, these effects are incorporated into the template. The subsequent use of the template will remove these time-dilation effects, whether artificial or genuine, from the new observations. Consequently, SALT2 calibrated light-curves cannot contain any cosmological data that is in the form of a power law.

The next step, illustrated by Figure 3, was to get the light-curves for four separate redshift ranges. Although

it was necessary to analyze the filter observations for each supernova in order to get the value of the peak flux density, its epoch, and the width for that filter, that width was not used to get the four light-curves. Although these light-curves have statistically significant width differences, there was no systematic trend that is consistent with time-dilation.

Analysis of the fitted widths as a function of intrinsic wavelength showed that they had a power-law exponent of $\beta = 0.171 \pm 0.055$ which is marginally consistent with no intrinsic wavelength dependence which because of equation 1, also implies no significant cosmological dependence.

The final part of the supernovae analysis was a regression of the light-curve width for each supernova and filter against $(1+z)$. For 1,070 data sets the raw exponent was $\alpha = -0.138 \pm 0.076$ and the intrinsic width corrected exponent was $\alpha = 0.038 \pm 0.075$. Both of these estimates are consistent with no time-dilation. If there is time-dilation the exponent must be one, which is inconsistent with these average widths at the 13σ level.

One way to validate these conclusions would be to redo the SALT2 analysis without the initial division of the epoch differences by $(1+z)$.

7.2. Gamma Ray Bursts

It has been shown that out to a redshift of $z = 8$, the GRB time duration variable T_{90} is consistent with no time-dilation but, because of the very large scatter of values, this result cannot exclude the possibility of time-dilation.

8. CONCLUSION

The final conclusion is that there is no support for an expanding universe with a standard time-dilation: all the results are completely consistent with no time-dilation which implies a static universe.

9. ACKNOWLEDGMENTS

This research has made use of the NASA/IPAC Extragalactic Database (NED) that is operated by the Jet Propulsion Laboratory, California Institute of Technology, under contract with the National Aeronautics and Space Administration. The calculations have used Ubuntu Linux and the graphics have used the DISLIN plotting library provided by the Max-Planck-Institute in Lindau.

APPENDIX

A. SOURCE OF SUPERNOVAE OBSERVATIONS

All of the original type Ia supernovae observations were retrieved from the SNANA (Kessler et al. 2009) in the download package *snana.tar.gz* on the website <http://www.snana.uchicago.edu> using the index files shown in Table 3. A current SALT2 template file for the JLA (Joint Light-curve Analysis) analysis was taken from the SNANA website

Table 3. Index source files for SNANA data

file
lcmerge/LOWZ_JRK07
lcmerge/JLA2014_CSP.LIST
lcmerge/JLA2014_CfAIII_KEPLERCAM.LIST
lcmerge/SNLS3year_JRK07.LIST
lcmerge/SDSS_allCandidates+BOSS_HEAD.FITS
lcmerge/JLA2014_SNLS.LIST
lcmerge/JLA2024_HST.LIST
lcmerge/SDSS_HOLTZ08

in the directory *models/SALT2/SALT2/JLAB14*.

The Pan-STARSS supernovae were accessed from the site https://archive.stsci.edu/prepds/ps1cosmo/jones_datatable.html.

Basic information for all the filters used is shown in Table 4 where column 1 is the filter name, column 2 is the mean wavelength in μm , column 3 (N1) is the raw number of supernovae with this filter, column 4 is the final number of supernovae with a valid light-curve for this filter, and column 6 is the HST filter name.

Table 4. Filter characteristics

Name	Wavelength ^a	N1	N2	HST
B	0.436	209	202	
V	0.541	211	158	
R	0.619	135	95	
I	0.750	149	96	
g	0.472	1,724	1,109	
r	0.619	1,766	1,019	
i	0.750	1,767	1,051	
z	0.888	1,705	928	
0	1.068	24	17	F110W_NIC2
1	1.555	6	0	F160W_NIC2
2	0.596	6	0	F606W_ACS
4	0.771	32	21	F775W_WFPC2
5	0.771	1	0	F775W_WFPC2
6	0.907	21	17	F850LP_ACS
9		1	1	F125W

^aWavelength in μm

B. SOURCE OF GRB OBSERVATIONS

The raw GRB data was taken from https://swift.gsfc.nasa.gov/archive/grb_table that had burst durations longer than 2 seconds and valid measurements for the redshift, T_{90} , the fluence and the peak one-second photon flux rate. The data labeled “Zhang” comes from Table 1 in Zhang et al. (2013).

REFERENCES

- Barthelmy, S. D., Barbier, L. M., Cummings, J. R., et al. 2005, *SSRv*, 120, 143, doi: [10.1007/s11214-005-5096-3](https://doi.org/10.1007/s11214-005-5096-3)
- Betoule, M., Kessler, R., Guy, J., et al. 2014, *A&A*, 568, A22, doi: [10.1051/0004-6361/201423413](https://doi.org/10.1051/0004-6361/201423413)
- Blondin, S., Davis, T. M., Krisciunas, K., et al. 2008, *ApJ*, 682, 724, doi: [10.1086/589568](https://doi.org/10.1086/589568)
- Conley, A., Guy, J., Sullivan, M., et al. 2011, *ApJS*, 192, 1, doi: [10.1088/0067-0049/192/1/1](https://doi.org/10.1088/0067-0049/192/1/1)
- Crawford, D. F. 2017, *Open Astronomy*, 26, 111, doi: [10.1515/astro-2017-0013](https://doi.org/10.1515/astro-2017-0013)
- Elias, J. H., Frogel, J. A., Hackwell, J. A., & Persson, S. E. 1981, *ApJ*, 251, L13, doi: [10.1086/183683](https://doi.org/10.1086/183683)
- Foley, R. J., Scolnic, D., Rest, A., et al. 2018, *MNRAS*, 475, 193, doi: [10.1093/mnras/stx3136](https://doi.org/10.1093/mnras/stx3136)
- Goldhaber, G., Groom, D. E., Kim, A., et al. 2001, *ApJ*, 558, 359, doi: [10.1086/322460](https://doi.org/10.1086/322460)
- Goobar, A., & Leibundgut, B. 2011, *Annual Review of Nuclear and Particle Science*, 61, 251, doi: [10.1146/annurev-nucl-102010-130434](https://doi.org/10.1146/annurev-nucl-102010-130434)
- Guy, J., Astier, P., Baumont, S., et al. 2007, *A&A*, 466, 11, doi: [10.1051/0004-6361:20066930](https://doi.org/10.1051/0004-6361:20066930)
- Guy, J., Sullivan, M., Conley, A., et al. 2010, *A&A*, 523, A7, doi: [10.1051/0004-6361/201014468](https://doi.org/10.1051/0004-6361/201014468)
- Holtzman, J. A., Marriner, J., Kessler, R., et al. 2008, *AJ*, 136, 2306, doi: [10.1088/0004-6256/136/6/2306](https://doi.org/10.1088/0004-6256/136/6/2306)
- Jones, D., Rodney, S. A., & Riess, A. G. 2013, in *American Astronomical Society Meeting Abstracts #221*, Vol. 221, 136.01
- Jones, D., Scolnic, D., Riess, A., et al. 2018, in *American Astronomical Society Meeting Abstracts #231*, Vol. 231, 308.06
- Kaiser, N., Burgett, W., Chambers, K., et al. 2010, in *Ground-based and Airborne Telescopes III*, Vol. 7733, 77330E
- Kessler, R., Becker, A. C., Cinabro, D., et al. 2009, *ApJS*, 185, 32, doi: [10.1088/0067-0049/185/1/32](https://doi.org/10.1088/0067-0049/185/1/32)
- Lien, A., Sakamoto, T., Barthelmy, S. D., et al. 2016, *ApJ*, 829, 7, doi: [10.3847/0004-637X/829/1/7](https://doi.org/10.3847/0004-637X/829/1/7)
- Meikle, P., & Hernandez, M. 2000, *Memorie della Societa Astronomica Italiana*, 71, 299. <https://arxiv.org/abs/astro-ph/9902056>
- Riess, A. G., Strolger, L.-G., Casertano, S., et al. 2007, *ApJ*, 659, 98, doi: [10.1086/510378](https://doi.org/10.1086/510378)
- Scolnic, D. M., Jones, D. O., Rest, A., et al. 2017, *ArXiv e-prints*. <https://arxiv.org/abs/1710.00845>
- . 2018, *ApJ*, 859, 101, doi: [10.3847/1538-4357/aab9bb](https://doi.org/10.3847/1538-4357/aab9bb)
- Zhang, F.-W., Fan, Y.-Z., Shao, L., & Wei, D.-M. 2013, *ApJL*, 778, L11, doi: [10.1088/2041-8205/778/1/L11](https://doi.org/10.1088/2041-8205/778/1/L11)